國立交通大學

生物醫學研究所

碩士論文

元件製程對於多晶矽奈米線場效電晶體水測電性影響之分析

Fabrication Process and its Effects on the Electric Characteristics of Poly Crystalline Silicon Nanowrie Field Effect Transistor in Aqueous Solution

研究生：魏若芬

指導教授：楊裕雄 博士

中華民國九十八年六月

元件製程對於多晶矽奈米線場效電晶體水測電性影響之分析

Fabrication Process and its Effects on the Electric Characteristics of

Poly Crystalline Silicon Nanowrie Field Effect Transistor in

Aqueous Solution

研究生：魏若芬　　　　　　　　　　　Student：Jo-Feng Wei

指導教授：楊裕雄 博士　　　　　　　　Advisor：Dr. Yuh-Shyong Yang

國 立 交 通 大 學

生 物 醫 學 研 究 所

碩 士 論 文

A Thesis
Submitted to Institute of Biomedical Science
College of Biological Science and Technology
National Chiao Tung University
in partial Fulfillment of the Requirements
for Degree of Master of Science
in
Biomedical Science

June 2009

Hsinchu, Taiwan, Republic of China

中華民國九十八年六月

元件製程對於多晶矽奈米線場效電晶體水測電性影響之分析

研究生：魏若芬　　　　　　　　指導教授：楊裕雄　博士

國立交通大學

生物科技學院　　　　　　生物醫學所

摘　　要

　　多晶矽奈米線場效電晶體生物感測器使用電訊號偵測生物分子具有極高靈敏度、即時偵測及無需標記物之優點。儘管矽奈米線場效電晶體具有以上的優勢，但是典型測試在水溶液電性變化影響之研究卻極少探討。在這裡，我們研究如何製作多晶矽奈米線場效電晶體以改善元件於水溶液環境下量測之電訊號穩定性。多晶矽奈米線場效電晶體於背閘極上，我們個別堆層二氧化矽及氮化矽兩種材料絕緣層及分析些兩種元件之電性號變化。同時使用新穎微流道保持水中環境並討論不同長度、不同條數之矽奈米線場效電晶體之水中電性測試。發現兩種材料作為絕緣層都具有極高的靈敏度與於水中測試之穩定度。最後，由於奈米線為矽材質，因此我們使用未固定化及固定化後之奈米線氮化矽作絕緣層元件測量不同pH值之PBS之關係。

Fabrication Process and its Effects on the Electric Characteristics of Poly Crystalline Silicon Nanowrie Field Effect Transistor in Aqueous Solution

Student：Jo-Fen Wei   Advisor：Dr. Yuh-Shyong Yang

Department of Biomedical Science
National Chiao Tung University

Abstract

Biosensors based on silicon nanowires promise real-time, highly sensitive and label-free electrical detection of biomolecules. Despite the tremendous potential and promising experimental results, the fundamental mechanisms of electrical sensing in aqueous environment remain poorly understood. In this work, we investigated how the fabrication process can help to improve the reliability of poly-Si nanowire filed-effect transistor (NWFET) in aqueous solution. Dielectric layers, silicon oxide or nitride, was prepared on the top of back gate in poly-Si NWFET and their effects on device characteristics were determined. The poly-Si NWFET was also prepared with variations of the number and length of the nanowires. The results indicated that either nitride or oxide dielectric layers as insulator improved the stability of poly-Si NWFET devices in aqueous solution. Finally, the pH effect on the electric properties of poly-Si NWFET was further investigated using unmodified and APTES modified device is nitride dielectric layer.

致　　謝

　　兩年半的研究生生涯對我來是一項大試煉，由於是跨領域學習，因此這段時間受到很多人的幫助。在修課及實驗的低潮期中總是可以聽到同學間互相鼓勵、打氣說：『加油』。聽到這句話後就可以帶著滿滿的信心把事情做完、做好。所以在研究生生活裡，我除了學習到寶貴的研究經驗外，更得到更多珍貴的友情。以及實驗室學長們對我這兩年半來照顧，因為你們讓我體會如何謙卑學習的心態、懂得心存感激、做任何一件事情不到最後別放棄…在此，我致上最誠心的感謝。

　　在此期間除了感謝我的指導教授 楊裕雄老師在學術與學術倫理方面的細心教導外，更感謝老師給我充足的實驗資源，讓我能進儀科中心、國家奈米元件實驗室(NDL)學習，並且給我自主學習的能力與及時的引導；同時感謝 林鴻志老師對我實驗上的一些寶貴意見及其研究室同學、學長、學弟、學妹在實驗上給予的幫助及鼓勵。還有國家實驗研究院　儀器科技研究中心提供專業的指導及NDL提供儀器及專業的工程師們，讓我們能夠在優質的環境下製作元件。

　　感謝電子所的維濤學弟提供論文修改寶貴的意見、行徽學長的細心指導、感謝小米學姐在實驗上給很多寶貴的學習經驗。在跨領域的學習階段中，特別的感謝宜貞及敏書同學一路上的貼心的鼓勵；感謝家人這兩年來的支持讓我無後顧之憂將碩士念完，以及過多提不完的你們。

　　你們是讓我完成碩論這個小成就中的最大推手，謝謝你們…同時，能夠認識你們，真是我的榮幸！

<div align="right">交通大學 生物醫學所 魏若芬 謹上</div>

CONTENTS

Table Captions

Chapter 1

Chapter 2

Chapter 3

Figure Captions

Chapter 2

Chapter 3

Appendix

Abbreviation

Poly Si	Poly Silicon
Single Si	Single Silicon
PDMS	Poly -(DiMethylSiloxane)
PBS	Phosphate Buffer Saline
pK_a	Acid dissociation constant
NW	NanoWire
SS	Subthreshold Swing

Chapter 1：Introduction

1-1 Background

There is increased demand for the availability of simple and reliable protocols for the

analysis of molecules of biological importance. The requirement of skilled manpower,

excessive external reagents, complicated sample preparation methods and time-consuming

procedures has limited the applications of most of the known classical techniques for different

bio-species detection (Table 1-1). [21] To address this critical issue, there are many studies in

biosensor recently. Biosensor is an analytical device which transforms the signal resulting

from the interaction of the analytes into the electrical signal that could be more easily

quantified and measured. One of the biosensors, poly-silicon nanowire field effect transistor

(Poly-SiNW FET) is important due to large surface-to-volume ratio, its electrical property

such as conductance is dominated by surface contributions. Therefore, the presence of

charged substance on the surface of an active nanowire induces a large fractional change in

the nanowire conductance and enables relatively easy detection. In other words, it possesses

ultrahigh sensitivity[22]. Besides, poly-Si NW FET is working by the label-free detection due

to the changes in electric response. Furthermore, it has more superior to others because of the

real-time detection.

Poly-Si NWFET can be prepared by either 'bottom-up' or 'top-down' lithography

approaches [6]. The top-down approaches typically employ advanced optical or E-beam

lithography tools to generate the NW patterns [13-14]. Although compatible with mass

production, the use of advanced lithography tools is costly. The bottom-up approaches usually

employ metal-catalytic growth for preparation of NWs [15-17]. However, the nanowires are

not easy to manipulate and arrange in order. For device fabrication with lift-off S/D formation,

it is also very difficult to fix the distance between source and drain. Hence, we fabricate

spacer poly-Si NWFET as sensor compatible with mass production as sensing device.

1-2 Motivation

In this work, we utilized a novel approach to release above concerns. The poly-Si

nanowire channels were fabricated by employing the poly-Si sidewall spacer technique,

which approach was comparable with current commercial semiconductor process and

forsaken expensive E-beam lithography tools. Though the poly-Si NWFET possesses

potential application for biological sensing application, there are still some drawbacks. For

instance the electrical characteristics of poly-Si NWFET are mainly influenced by the

defects in the grain boundaries and within the grains [18]. Trap states resulted from those

defects within the channel lead to poor device performance, such as low field effect

mobility, large leakage current [19], large subthreshold slope, and high threshold voltage.

Another issue is the stability for testing in aqueous solution which is very essential for

development of advanced biosensor technology. The design of reliable biological or

chemical sensors, which principle is based on the detection of changes in the surface

charges, requires reducing the influence of any unwanted or uncontrolled potential-induced charging at the substrate-bio layer interface. Because of the leakage current in the test solution is unstable during measurements; it may also affect the electrical characteristics of NW devices. To address this critical issue, we improve water-tested reliability of poly-Si NWFET by using a stacked dielectric consisting of nitride layer [20]. Besides, we prepare different pH phosphate buffer saline (PBS) solutions (see in appendix 1) and then measured the electric portieres of the test devices. The phenomenon of the tested devices is measured and analyzed.

1.3 Thesis Organization
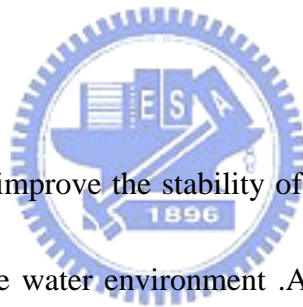
This thesis is focused on improve the stability of poly-Si NWFET for the measurement of the electrical property in the water environment .Additionally, we compare the electrical property of three devices that fabricated by a stacked dielectric either of oxide layer and nitride layer. This thesis is divided into four chapters.

Chapter 1： Introduce and descript strong points of the spacer NWFET character and some issues for bio test to improve.

Chapter 2： Review describes the MOSFET classical electrical property definition and the fabrication of microfluidics is described.

Chapter 3：Detail description of device fabrication and data.

Chapter 4 ： Brief insight of the results obtained.

References：

[1]G.M. Laws, T.J. Thornton, Jinman Yang, L.de la Garza, M. Kozicki, D.gust, Phys. Stat. sol.(b) 233,83-89.

[2] F. Davis, A.V. Nabok, S.P.J. Higson, 2005. *Biosens, Bioelectron.***20**, 1531-1538.

[3] R.J. Mitchell, M.B. Gu, 2004. *Biosens. Bioelectron*. **19** ,977-985.

[4] Besteman, K., Lee, J., Wiertz, F.G.M., Heering, H.A., Dekker, C., 2003. *Nano Lett*. **3**, 727–730.

[5] Cui, Y.,Wei, Q., Park, H., Lieber, C.M., 2001. *Science* **293**, 1289–1292.

[6] Li, C., Curreli, M., Lin, H., Lei, B., Ishikawa, F.N., Datar, R., Cote, R.J., Thompson, M.E.,Zhou, C., 2005. *J. Am. Chem. Soc*. **127**, 12484–12485.

[7] Hahm, J., Lieber, C.M., 2004. *Nano Lett*. **4**, 51–54.

[8] Patolsky, F., Zheng, G., Hayden, O., Lakadamyali, M., Zhuang, X., Lieber, C.M., 2004. *PNAS* **101**, 14017–14022.

[9] Patolsky, F., Zheng, G., Lieber, C.M., 2006c. *Nanomedicine* **1**, 51–65.

[10] Star, A., Tu, E., Niemann, J., Gabriel, J.C.P., Joiner, C.S., Valcke, C., 2006. *PNAS* **103**, 921–926.

[11] Wang,W.U., Chen, C., Lin, K., Fang, Y., Lieber, C.M., 2005. *PNAS* **102**, 3208–3212.

[12]Chen, Y., Wang, X., Hong, M.K., Erramilli, S., Mohanty, P., Rosenberg, C., 2007. *Appl. Phys. Lett*. **91**, 243511.

[13] Lee, K.N., Jung, S.W., Kim, W.H., Lee, M.H., Shin, K.S., Seong, W.K., 2007. *Nanotechnology* **18**, 445302.

[14] Li, Z., Chen,Y., Li, X., Kamins, T.I.,Nauka, K., Williams, R.S., 2004.*Nano Lett.* **4**, 245–247.

[15] Duan, X., Huang, Y., Lieber, C.M., 2002. *Nano Lett*. **2**, 487–490.

[16] Duan, X., Niu, C., Sahi, V., Chen, J., Parce, J.W., Empedocles, S., Goldman, J.L., 2003.*Nature* **425**, 274–278.

[17] McAlpine, M.C., Friedman, R.S., Jin, S., Lin, K.H.,Wang,W.U., Lieber, C.M., 2003. *Nano Lett.* **3**, 1531–1535.

[18] Wu, I. W., Jackson, W. B. T., Huang, Y. A., Lewis, G., and Ciang, A., 1991. *IEEE Electron Device letter* **12**, 181-183.

[19] Fossum, J. G., Ortiz-Conde, A., Shicjijo, H., Banerjee, abd S. K., 1985. *IEEE Trans. Electron Devices* **32**, 1878-1882.

[20] Hsiao, C.Y., Lin, C.H., Hung, C.H., Su, C.J., Lo,Y.R. Lee,C.C., Lin, H.C., Ko,F.H., Huang,T.Y., Yang,Y.S. 2009. *Biosensors and Bioelectronics* **24**, 1223-1229.

[21] Arora, K., Chand, S.,Malhotra, B.D.,2006. *Analytica Chimica Acta* ,**568**, 259-273.

[22]Chen,Y., Wang, X., Erramilli, S., Mohanty, P., 2006. *Appl. Phys. Lett.*,**89**. 223512-1-223512-3.

Table 1- 1 Comparison chart with various sensing methods. [21]

Detection technique	Assay time	Limitations of technique
Molecular biological methods / Biochemical methods	1–3 days	Longer assay time
Serological tests or Immunological detection Methods	1–2 days	Costly, requirement of monoclonal antibodies, longer assay time, etc.
Western blotting	1–2 days	Costly, longer assay time, skilled manpower
Gas sensing methods (GC, HPLC,etc.)	2–3 hr	Costly, no on-site measurement
Polymerase Chain Reaction	~2–4 hr	No on-site detection, need of enrichment, etc.
Nucleic acid sequence-based Amplification (NASABA)	<1 hr	On-site testing can not be performed
Immune diagnostic kits	Within minutes to hours	Costly
DNA probe assay		Longer assay time, pre-enrichment, various pre-experimental preparations, etc.
Fourier transform infrared and Raman spectroscopy	~5–10 min	Costly and complicated instrumentation

Chapter 2：Measurement Setup and Microfluid System

2-1 Microfluidics Fabrication

We proposed one method to set up our microfluidics that can be reused on different test chips. The apparatus of the use of the technique is shown in Fig. 2-1. The PDMS poly-(dimethylsiloxane) has been one the most actively developed polymers for Microfluidics. The semi-structural formula of this material is show in Fig.2-3. Table 2-1 lists its chemical and physical properties, those which are feasible for fabrication of devices with useful functionality.

Below is the microfluid system process flow[2]：

1) Maxing PDMS (poly dimethylsiloxane)：volume ratio = 10:1 with stirring rod for

   5min

2) Use vacuum pump to degas about 20 min until most bubbles are gone

3) Pour it to a mother mode (glass)

4) Cure PDMS at 90°C for 20 min

5) Carefully peel off the PDMS structure

6) Punch input and output holes

7) Surfaces may need to be cleaned with acetone.

8) Bond PDMS microfluid system to nanowire devices

9) Bake with oven at 90°C for 30 min

10) Align and press them together

11) Insert Teflon tubes to inject sample with string pump

12) Test and measure completed samples. (Fig 2-2)

2-2 Method of Device Parameter Extraction

In this thesis, we use N&K1500 to measure the thickness of amorphous-Si, TEOS oxide and nitride films in the fabrication procedure. All the electrical characteristics of proposed poly-Si FETs were measured by Keithley 2636 System SourceMeter Instrument. See the way below that are used for extracting the electrical parameters of the NW devices.

2-2-1 Determination of the Threshold Voltage [3]
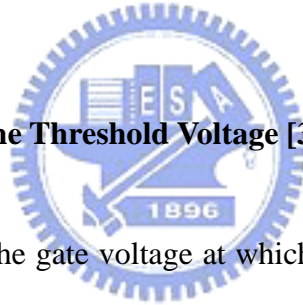
For bulk MOSFET, the gate voltage at which the electron density at the interface is the same as the hole density in the neutral bulk material is called the threshold voltage [6]. For an n-channel device as the gate voltage is above the threshold voltage, the transistor is turned on due to the induction of a sheet of electrons in the channel at the oxide-silicon interface creating a low-resistance channel where charges can flow from drain to source.

For NW devices, the body effect can be ignored, and the MOSFET current-voltage equation is

$$I_D = k[V_{GS} - V_T - I_D r_s - 0.5(V_{DS} - I_D(r_s + r_D))][V_{DS} - I_D(r_s + r_D)] \qquad (2\text{-}1),$$

where r_S and r_D are defined in Fig. 2-4. Threshold voltage can be extracted using the linear extrapolation method. In this method, the drain current is measured as a function of gate voltage at a low drain voltage (typically 50mV) to ensure operation in the linear MOSFET region. Because of series resistance is usually negligible at the low drain currents where threshold voltage measurements are made. According to Eq. (2-1), as the drain current is zero, we can express Eq. (2-2) in terms of V_{GS} and V_D:

$$V_{GS} - V_T - 0.5V_D = 0 \qquad\qquad (2\text{-}2).$$

But Eqs. (2-1) and (2-2) are valid only above threshold. The drain current is not zero below threshold and approaches zero only asymptotically. Hence in this method the I_D verus V_{GS} curve is extrapolated to I_D=0 and the threshold voltage is determined from the extrapolated or intercept gate voltage V_{GSi} by

$$V_T = V_{GSi} - \frac{V_{DS}}{2} \qquad\qquad (2\text{-}3).$$

In this work, we use another way which is simpler than the complex linear extrapolation method to extract the threshold voltage. In this method, the threshold voltage is defined as the gate voltage as the drain current is specified at (W/L) $\times$10nA for V_{DS}=0.1V and (W/L) $\times$100nA for V_{DS}=5V, where W and L are channel width and channel length, respectively.

2-2-2 Determination of Subthreshold Swing

Subthreshold swing, S.S. (V/dec), is a typical parameter to describe the control ability of gate voltage. For an ideal switch device, it is turned off as the gate voltage is below the threshold voltage and ideally there is no current from the drain to the source. In reality, there is a current, dubbed subthreshold current (or leakage), flows along the channel although it is relatively small and varies exponentially with gate bias. Subthreshold swing is defined as the amount of gate-voltage shift required to modulate the subthreshold current by one oreder of magnitude. The exact S.S. can be extracted using the following formula: [4]

$$SS = (\frac{\partial \log_{10}^{(I_D)}}{\partial V_G})^{-1} \qquad\qquad (2\text{-}4).$$

According to Eq.(2-4), the lower the S.S. is, the better the gate controllability does. For bulk CMOS devices, the value typically falls in the range from 60 to 90mV/dec. For polycrystalline-channel devices, however, the value is typically much larger due to the existence of abundant defects in the channel.

2-2-3 Determination of the On/Off Current Ratio

High On/Off ratio represents high signal (on current) to noise (off-state leakage current) immunity. In this study, the on(drive) current and off(leakage) current are defined as the maximum and the minimum drain current recorded in the transfer curve.

The leakage current is considered as one of the main problems on poly-Si NWFET. Because of the poly-Si NWFET is composed of polycrystalline channels which contain a large amount of defects in grain boundaries. These defects serve as trap states for conduction carriers in energy band gap. As the device is turned off and the voltage difference between the gate and drain is sufficiently high, those traps act as centers to enhance band-to-band tunneling process and thus the off-state current. Therefore there are many studies in poly-Si to improve the grain structure [7-8]. Here we defined the on/off ration as blow.

$$\frac{I_{ON}}{I_{OFF}} = \frac{\text{Max. current of } I_{DS}\text{ - }V_{GS} \text{ plot at } V_{DS} = 0.5V}{\text{Min. current of } I_{DS}\text{ - }V_{GS} \text{ plot at } V_{DS} = 0.5V} \qquad (2\text{-}5).$$
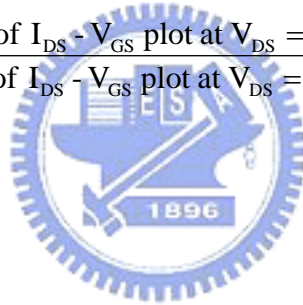
References：

[1]Mc Donald, J., Whitesides, G., 2002 Accounts of chemical research, 35,491-499.

[2]Wang, T.M. (2007, June). "Study of nanowires thin-film-transistor for biochemical sensor applications",National Chiao Tung University, Hsinchu.

[3]Schroder, D.K. (1990), "Semiconductor material and device characterization," John Wiley & Sons, New York, pp 81-82.

[4]Cristoloveanu, S., Blalock, B., Allibert, F., Dufrene, B.M., and Mojarradi, M.M., "The Four-Gate Transistor," Proc. ESSDERC'02, 323-326, 2002.

[5]Levinson, J., Shepherd, F. R., Scanlon, P. J., Westwood, W. D., Este, G., and Rider, M.,1982. *J. Appl. Phys.*,**53**, 1193–1202.

[6] Sze, S. M.,(1981), "Physics of semiconductor devices" 3rd edition, John Wiley & Sons, New York, pp 312.

[7] Song, I.H., Kim, C.H., Nam,W.J., and Han, M.K.,2002. *in IEDM Tech. Dig.*, pp. 561–564.

[8] Lee, S.W., Ihn, T.H., Joo, S.K.,1996. *IEEE Electron Device Lett* **17**,407-409.

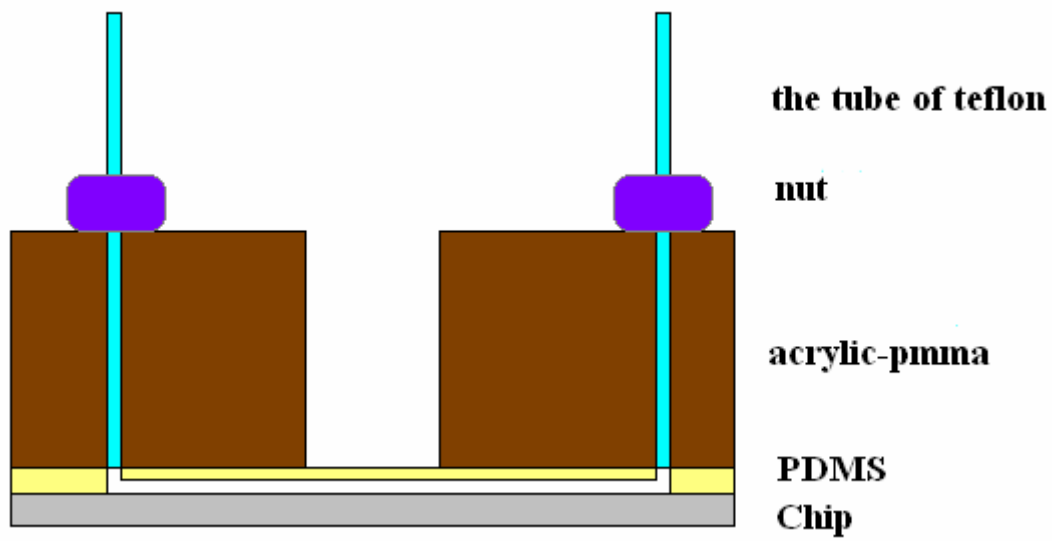Figure 2- 1：The diagram is the cross-section of Microfluidics apparatus.

Figure 2- 2：Microfluidics apparatus.
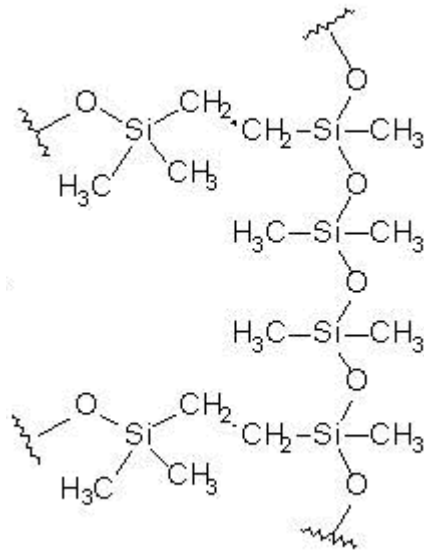
Figure 2- 3： Semi-structural formula of PDMS.
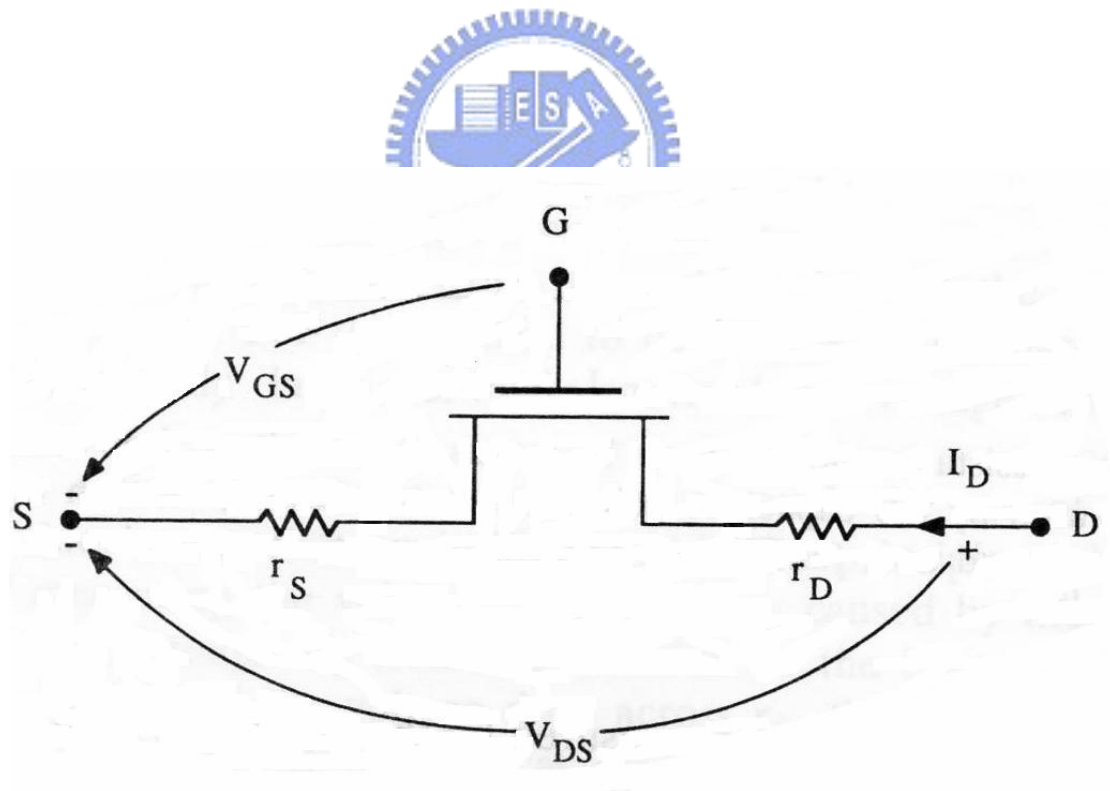
Figure 2- 4： A MOSFET with source and drain resistances [3]

Table 2- 1：Physical and Chemical Properties of PDMS

Property	Characteristic
Density	Around 0.9kg/m^3
Optical	Trnsparent, between 300nm and 2200nm
Electrical	Insulating, breaking filed 20kV/cm
Mechanical	Elastomeric, Young's modulus ~ 750kPa
Thermal	Insulating, thermal conductivity ~0.2W/m/K
Interfacial	Low surface energy (~20 mN/m)
Permeability	Permeable to gas, apolar organic solvents, nearly impermeable to water
Reactivity	Inset, oxidizable by plasma
Toxicity	Non-toxic

Chapter 3：Fabrication and Electrical Characterization of Nanowire

Transistors

The silicon surface, after a wet treatment or an oxidation step, appears hydrophilic. Actually as a Si wafer is placed in a normal environment an oxide layer with thickness between 0.6 and 2nm would be formed at the surface. However, quality of this native oxide is poor with typical dangling bond defect density in the range of 10^{12} cm^{-2} at Si/oxide interface. The defect densities reported are about two orders of magnitude higher than that for thermal oxides. [1] In our work, the poly-Si nanowaires expose either in the air or in the solution directly. That will produce native oxide which may bring about concerns about the traps and associated leakage issue. In this chapter, we state the fabrication process and electrical characteristics of poly-Si NWFET with variations of the number and length of the nanowires such as on current, subthreshold swing, threshold voltage in the environment that either in the air or solution. We can see the on current is simply proportional to the number of NW channels.

3-1 Device Structures and Fabrication

Our experiments employed NWFETs fabricated on 6-inch p-type wafer capped with a dielectric layer, either a thermal oxide layer or a nitride/oxide stacked layer. Figs. 3-1(a) and (b) show the top (layout) and cross-sectional views (along the A – B direction in Fig. 3-1(a)),

respectively, of the device, dubbed as device A, formed on the thermal oxide layer. Similar views for the device, denoted as Device B, formed on a nitride/oxide stacked layer are shown in Fig. 3-2. In these devices the poly-Si NWs are formed by means of sidewall spacer etching technique.

In Fig.3-1, the fabrication began on Si wafers capped with a 100 nm-thick thermal oxide. Next, a 100nm-thick nitride layer was deposited by low-pressure chemical vapor deposition (LPCVD). After deposition of the nitride layer, standard photolithographic and etch steps were performed to form the nitride dummy structures. Subsequently, a 100nm-thick amorphous-Si layer was deposited and then anneal at 600°C for 24hr in N_2 ambient to transform it into polycrystalline. Afterwards, source/drain (S/D) doping was done with phosphorus ion implantation with a dose of $5E15cm^2$. After the generation of S/D photoresist patterns with a lithographic step, a reactive plasma etching step was performed to form the S/D regions. Owing to the anisotropic etching process, poly-Si NW channels were formed at the nitride dummy structure simultaneously during the S/D etching step. By carefully controlling the etching time, the cross-sectional dimensions of poly-Si NW channels can be easily reduced to sub-100 nm scale. Subsequently, all devices were then covered with a 200-nm-thick TEOS oxide passivation layer. Finally, removed by a 2-step dry/wet etching process to expose the poly-Si NW.

Note that the wet etching rate of TEOS oxide in the lift step was adjusted to a low value.

Because of device could be short in our water tested.

Fabrication of device B began on Si wafers capped with a 100nm-thick thermal oxide. First 50nm-thick nitride and 100nm-thick TEOS oxide layers were sequentially deposited by LPCVD. Next was the formation of the TEOS dummy structure. Subsequently, the 100nm-thick amorphous-Si layer was deposited on the dummy gate and anneal at 600°C for 24hr in N_2 ambient to transform poly-Si respectively. Then source/drain (S/D) doping was performed with phosphorus ion implantation with a dose of 5E15cm^2. After the generation of S/D photoresist patterns with a lithographic step, a reactive plasma etching step was performed. Owing to the anisotropic etching process, poly-Si NW channels by the side of the nitride were formed simultaneously during the S/D etching step. Subsequently, all devices were then covered with a 200-nm-thick TEOS oxide passivation layer. Finally, removed by a 2-step both dry and wet etching process to expose the poly-Si NW. The cross-sectional and top SEM images of a poly-Si NWFET with NW channels as thin as 33nm to 60 nm are shown in Fig.3-3(a) and (b), respectively.

In this work the substrate serves as the bottom-gate for electrical measurements of the NW devices. Thickness and quality of the dielectric layer capped on the Si wafer would thus affect the device performance. For more flexibility, we also fabricated device C which has a 150nm-thick nitride layer as the capping insulator. Its structure is shown in Figs. 3-4 (a) and (b), which are the top (layout) and cross-sectional views (along the A – B direction in Fig. 3-4

(a)), respectively, of the device.

3-2 Effect of Electric Properties of Device in either Water or Air

It is known that the existence of grain boundaries within the poly-Si channel region has great influence on the electrical characteristics of poly-Si device. [2] Those defects may act as trap centers for conductive carriers and give rise to potential barriers which impede the flow of current from one grain to another. [3] For biological sensors, the defects could also affect the sensitivity degradation.In a recent paper the water passivation effect was reported to reduce such influence while the poly-Si NWFET is immersed and operated in the water environment [4]. The DI water possesses abundant H^+ and /or OH^- which may diffuse into the grain boundaries and terminate on the dangling bonds wherein. [4] Such action may passivate the defects and thus the electrical characteristics are improved.

Here, we investigate the phenomenon by comparing the electrical characteristics of the poly-Si NWFET measured either in the water or in the air. Figure 3-5 shows the process flow of the test. The characteristics (I_{DS}-V_{GS}) of device A, device B and device C measured in various environments are shown in Fig. 3-6, Fig. 3-7 and Fig. 3-8, respectively (V_D=0.5V). As can be seen in the figures, the electrical characteristic of the poly-Si NWFET in the water is significantly improved in terms of reduced threshold voltage and subthreshold swing. Therefore, we believe that trap states were effectively reduced by water passivation. As the Fig.3-8, we also can observe the effect of vacuum drying on the device performance. Such

vacuum treatment is 30 min. It is clearly seen that the threshold swing is significantly higher

than that before vacuuming that shown in Fig. 3-19. We suspect that the vacuum treatment

tends to draw out the hydrogen atoms from the poly-Si; therefore the device characteristics

are degraded. For fresh devices, some hydrogen species which has been contained in the

poly-Si are believed to come from the underlying SiN which was deposited with H-related

reaction gas (e.g., SiH_4 and NH_3), thus abundant of hydrogen atoms are incorporated in the

SiN film [5]. Portion of the H species diffuse into the poly-Si nanowire and passivate the

defects existing therein in the subsequent process steps, thus the fresh device show improved

performance. Owing to the high difference in pressure between the environment and the grain

boundary space that hydrogen may desorbs and release to the environment, thus the device

performance is dramatically degraded. As the test device is placed in the water, the water

passivation occurs to recover and improve the device characteristics.

3-3 Effect of Channel Length and Number on the Electric Properties of Poly NWFETs

Figure 3-9 to Fig. 3-12 show the measured results of device C. Figure 3-9 and Fig.

3-11 show the transfer characteristics (I_{DS}-V_{GS}) of devices with different channel number

measured in the air and water, respectively. The summary of normalized drain current as

function of channel number (to a single-channel device) is shown in Fig.3-9 and

summarized in Table 3-1. The normalized on current is extracted at V_G-V_{th} = 0.7V and

V_D=0.5V. The results are reasonable since the drain current is proportional to the number of

NW channels, indicating that the NW channels exhibit stable and uniform operation

characteristics. This is especially true in water (see Fig.3-9 and Table 3-1), owing to the

high k value (78.5) of the water as well as the water passivation effect [10]. Figure 3-10 and

Fig. 3-12 shows the transfer characteristics of devices with different channel length

measured in the air and water, respectively. The extracted threshold voltage and

subthreshold swing of device C are shown in Table 3-2. In theory, we could see the

threshold voltage and subthreshold swing decreased with the length of channel. Because of

the dry etching could not produce uniform size of channel width, as can be seen the Fig. 3-2.

Hence the resistance of the channel has some variation for our expected. But the data shown

in Table 3-2 still quite near mutually.
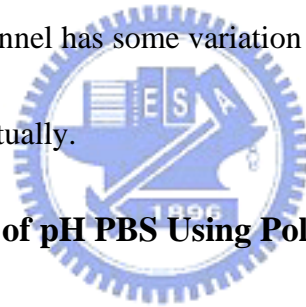
3-4 Sensing Measurements of pH PBS Using Poly-Si NWFETs

Many works have been reported on sensing the pH of a solution using nanowire FETs.

[6-9] However, in those works the NW channel materials are single crystal. Here, we measure

the electrical properties of different pH PBS by the fabricated NW devices. Here we select

device C-type for the measurements, because among the three types of devices characterized

in previous section, device C is found most reliable and reproducible.

Figure 3-13 to Fig.3-15 show the sensing characteristics (I_D-Time) for PBS (10mM) of

different pH. The test system is illustrated in Fig.3-16. As mentioned above, poly-Si materials

contain grain boundaries that not exist in single-Si, and the extra defects may affect the

electrical characteristics. Fortunately, such concern could be lifted with the water passivation effects [4]. As has been confirmed in this work, the electrical properties of the fabricated NWFETs are stable in either air or water. As evidenced in Figure 3-6 and Fig. 3-7 and Fig. 3-8, the characteristics of poly-Si NWFETs are improved and reproducible in the water-tasted environment. One report describes that the fluid surrounding the nanowire sensor can significantly affect the detection results with two factors. One is the electrostatics of the test device due to the fringing-induced barrier. The other is the amount of charge induced on nanowire.[10] For example, for the n-type channel devices tested in this work, negative carries attached on the nanowire surface would affect the device's threshold voltage. Deionized water is usually slightly acidic because of the dissolved carbonic acid that it picks up from the atmosphere. Therefore, deionized water will have a pH around 5 to 6 when exposed to the air [11]. This chemical response is shown in below equation：

$$CO_2 + H_2O \rightarrow H_2CO_3$$
$$H_3CO_3 \rightarrow HCO_3^- + H^+$$
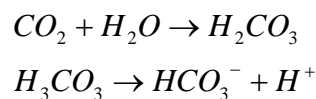
Moreover, the pK_a (see appendix 2) of the silicon oxide is 6.8. Hence, the higher density of charges presenting in the solution than in the air, we expect that the threshold voltage shift due to the variation of the test solution should be more significant than in the air.

The silicon surface after wet handling that could produce the thickness between 0.6-2.0 nm oxide-layer. Because of the silicon oxide possess the pK_a =6.8. At high pH, -SiOH is deprotonated to –SiO⁻, which correspondingly cases a decrease in current. The chart is shown

in Fig. 3-17. [12] To support this point, we carried out real-time pH-drain current

measurements on unmodified poly-Si NWFET. The results are shown in Fig. 3-13 to 3-14. To

test the reproducibility of the pH sensor, measurements under varied pH values were

repeatedly performed on a device. In addition we've also modified the poly-Si nanowire with

APTES(see in appendix 3), which produces amino groups, moreover, the amide group can

produce the other pK_a(3.9).[13] Therefore, with the APTES treatment, we can extend the

measurements to solutions with a low pH value. The SiNW surface illustrating changes in the

surface charge state with pH is shown in Fig.3-18. [7] The data for modified poly-Si nanowire

are shown in Fig. 3-15. As expected [7] [8], the test devices with APTES-modified nanowire

surface show more steady performance than the unmodified one, especially while we

pumping PBS with a faster rate.
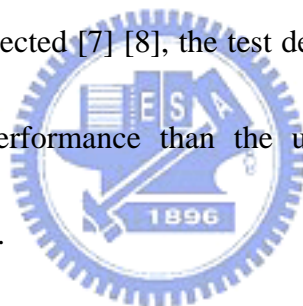
References：

[1]Okorn-Schmidt H.F.,1999. *IBM J. res. develop.* **43**,351-365.

[2]Fossum ,J. Ortiz-Conde, G. A., 1983. *IEEE Trans. Electron devices*, **30**,933-940.

[3]Baccarani,G., Ricco, B.,Shchini,G.,1978. *J Appl. Phys.*,**49**, 556-5570.

[4]Lin, H.C., Su, C.J., Huang, T.Y., 2007. *Appl, phys, Letters*,**91**.v 202113-1-202113-3.

[5] M. Shimaya, *Proc. Int. Reliability Physics Symp.*, pp.292-296, 1995.

[6]Stern,E., Klemic,J. F., Routenberg, D. A., Wyrembak, P. N., Turner-Evans
   D.B.,Hamilton ,A. D., LaVan, D. A. , Fahmy, T. M. & Reed ,M. A.,2007. *Nature,* 445.
   519-522.

[7]Cui, Y., Wei, Q., Park, H., Lieber, C.M.,2001. *Science*, **293.**   1289-1292.

[8]Chen,Y., Wang, X., Erramilli, S., Mohanty, P., 2006. *Appl. Phys. Lett.*,**89**.
   223512-1-223512-3.

[9]Laws, G.M., Thornton, T.J., Yang, Garza, L.de la, Kozicki,M., Gust, D.,2002. *Phys. Stat.*
   sol.(b) **233**. 83-89.

[10]Nair, P.R., Alam, A.,2007. *IEEE Transactions on electron devices* **54**. 3400-3408.

[11] Leo M. L. Nollet (2000). *Handbook of water analysis.* (pp 70-71) CRC Press.

[12]Chua, L.L.,Zaumsell, J., Chang, J.F., Ou, E.C.-W., Ho, P.K.-H., Sirringhaus, H.,Friend,
   R.H.,2005. *nature* **434.** 194-199.

[13] Vezenov, D. V., Noy, A., Rozsnyai, L. F., Lieber, C.M., 1997. *J. Am. Chem. Soc.***119**.
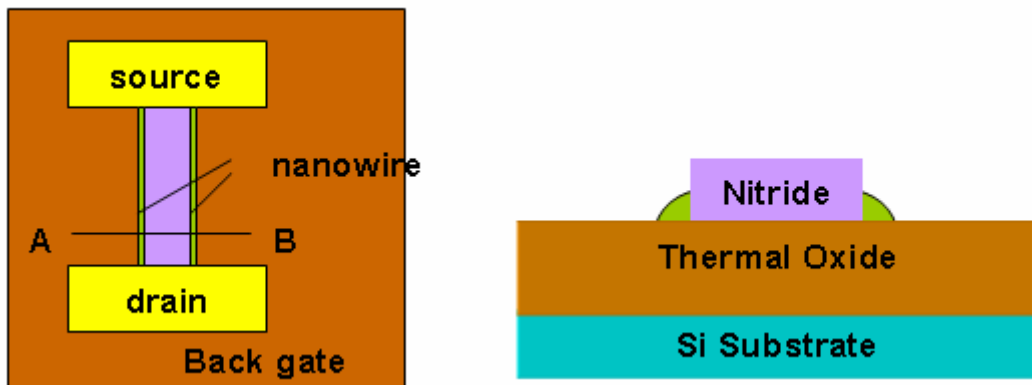   *2006-2015.*

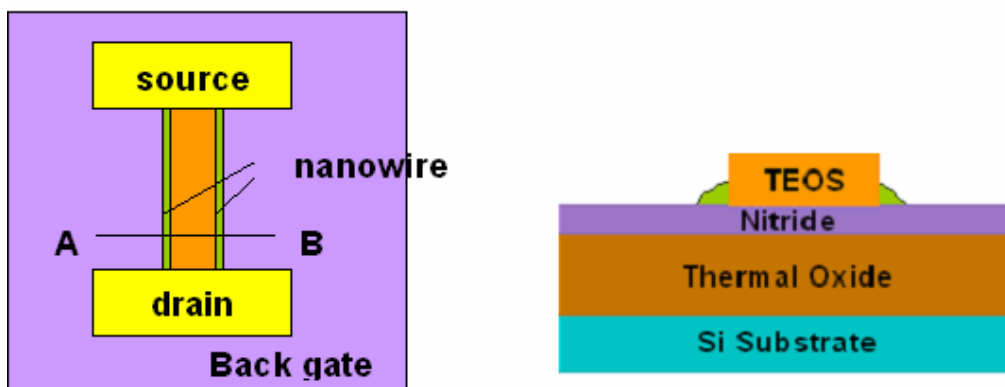Figure 3- 1：Device A (a) Top and (b) cross-sectional views of the stacked dielectric oxide layer poly-Si NWFET .

Figure 3- 2：Device B (a) Top and (b) cross-sectional views of the stacked dielectric nitride and oxide layer poly-Si NWFET .
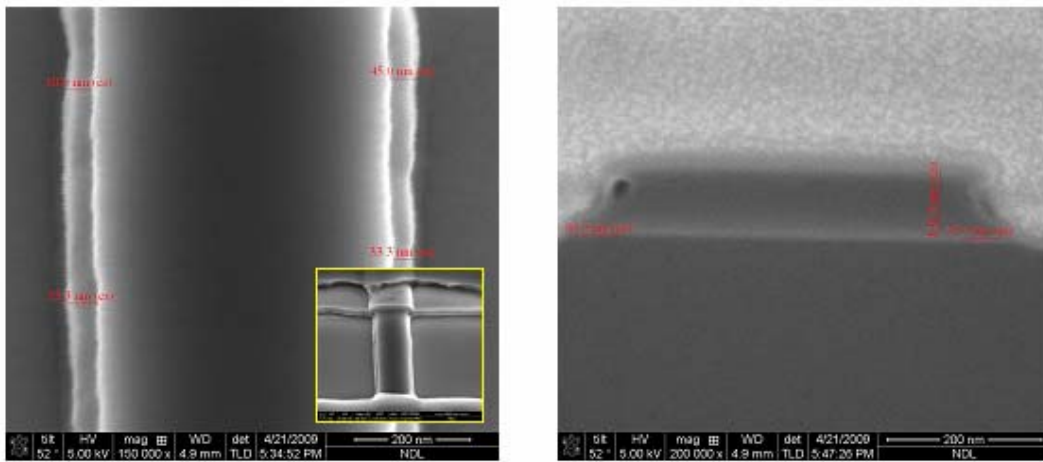
Figure 3- 3： (a) Top and (b) cross-sectional SEM images of poly-Si NWFET which NW channel as thin as 33-60nm wrapped by the spacer-wall.
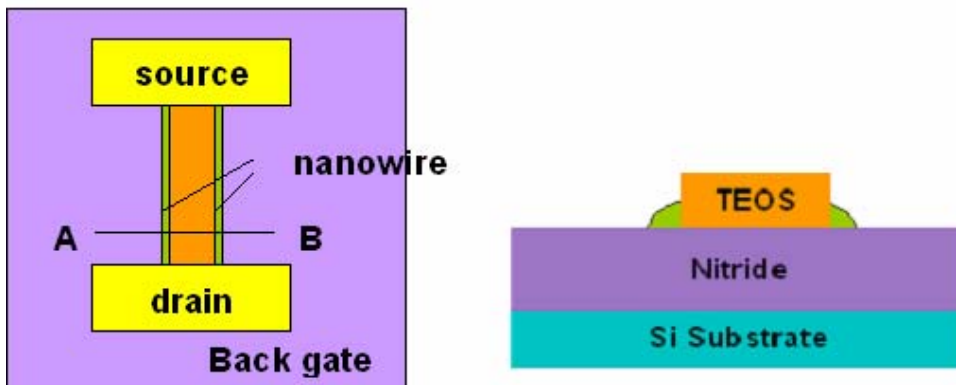

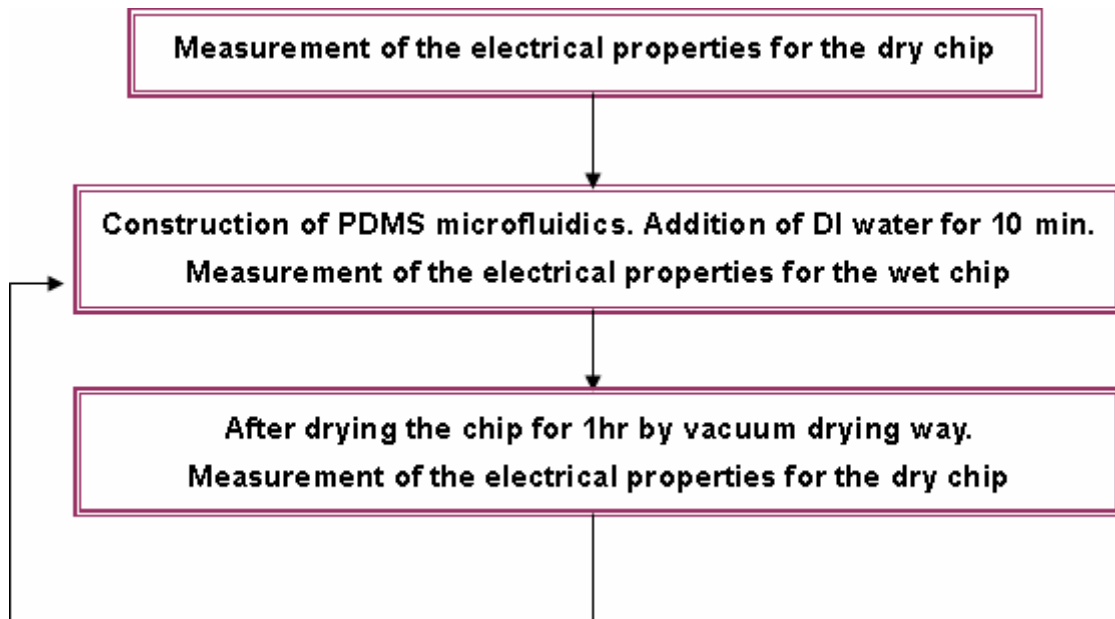Figure 3- 4：Device C (a) Top and (b) cross-sectional views of the stacked dielectric nitride layer poly-Si NWFET.

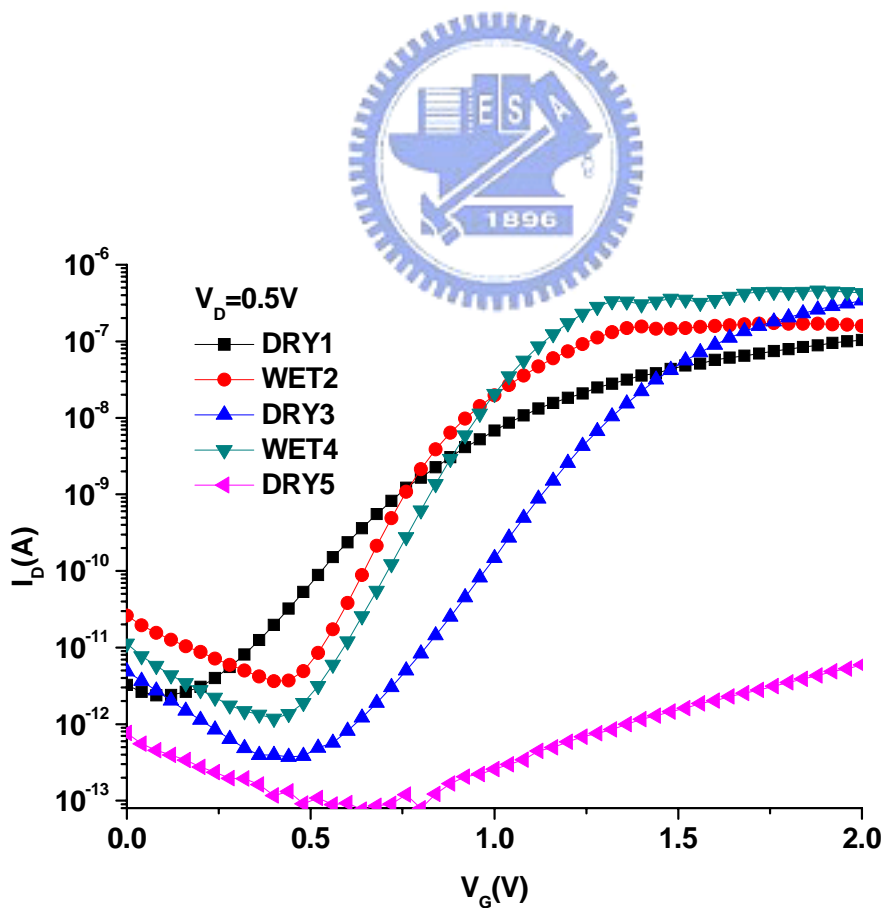Figure 3- 5：The process steps for measurement of the electrical properties of the nanowire devices.

Figure 3- 6：The electrical properties of the stacked dielectric oxide layer poly- Si NWFET (Device A) measuring in the air and water.
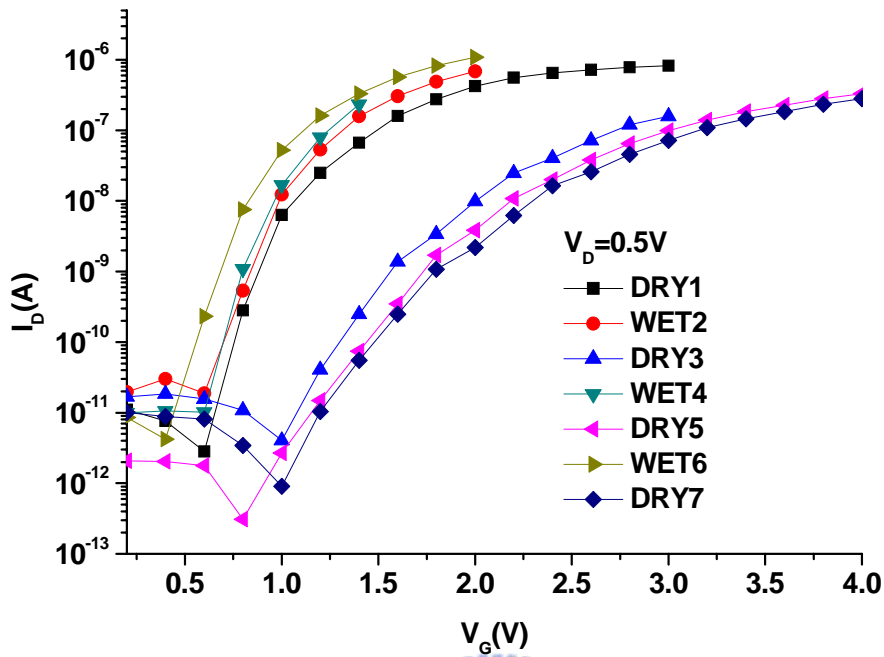
Figure 3- 7：The electrical properties of the stacked dielectric nitride and oxide layer poly-Si NWFET (Device B) measuring in the air and water.
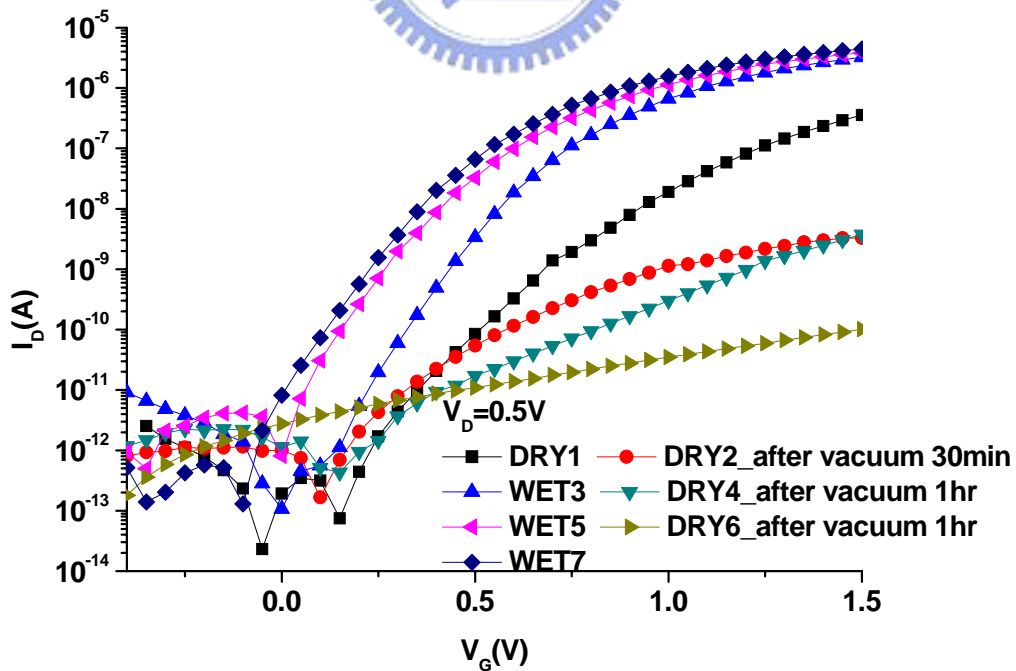

Figure 3- 8：The electrical properties of the stacked dielectric nitride layer poly-Si NWFET (Device C) measuring in the air and water.
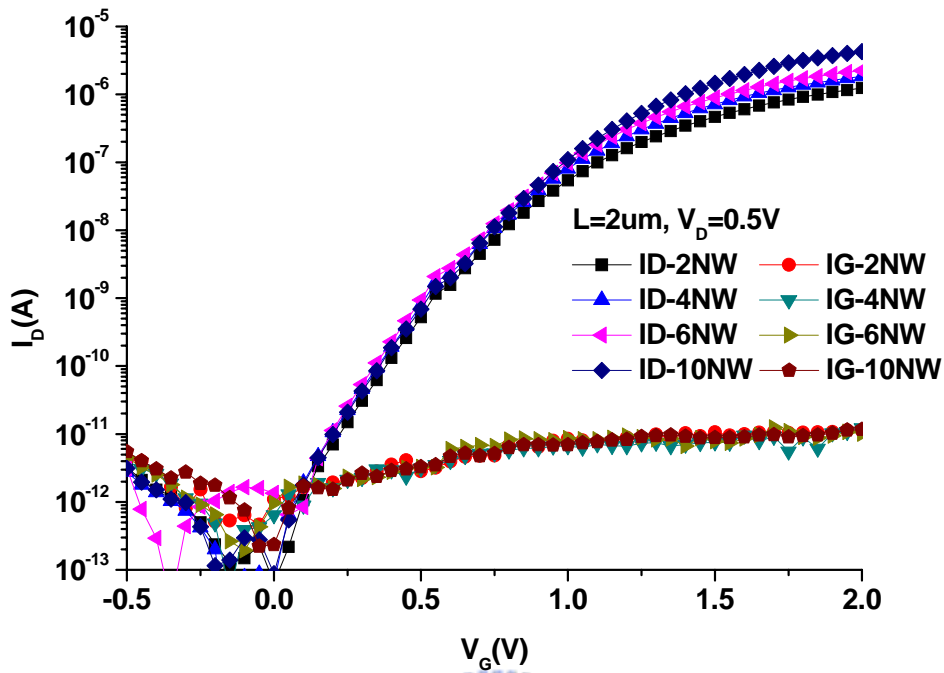
Figure 3- 9：Transfer characteristics of the proposed the stacked dielectric nitride layer poly-Si NWFET (device C) with difference channel that measures in the air.
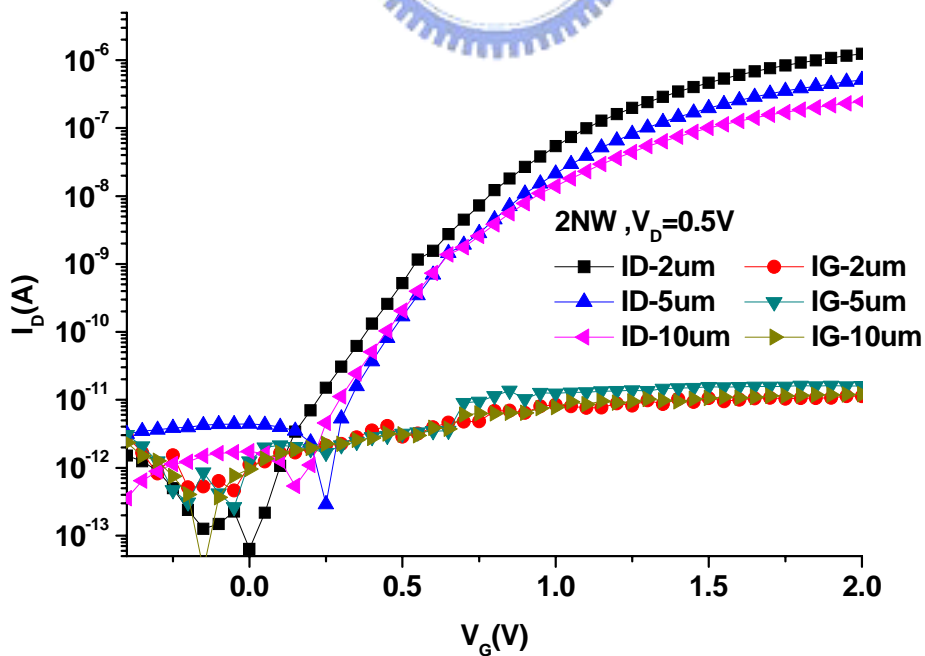

Figure 3- 10：Transfer characteristics of the proposed the stacked dielectric nitride layer poly-Si NWFET (device C) with difference length that measures in the air.

Figure 3- 11：Transfer characteristics of the proposed the stacked dielectric nitride layer poly-Si NWFET (device C) with difference length that measures in the water.

Figure 3- 12：Transfer characteristics of the proposed the stacked dielectric nitride layer poly-Si NWFET (device C) with difference length that measures in the water.
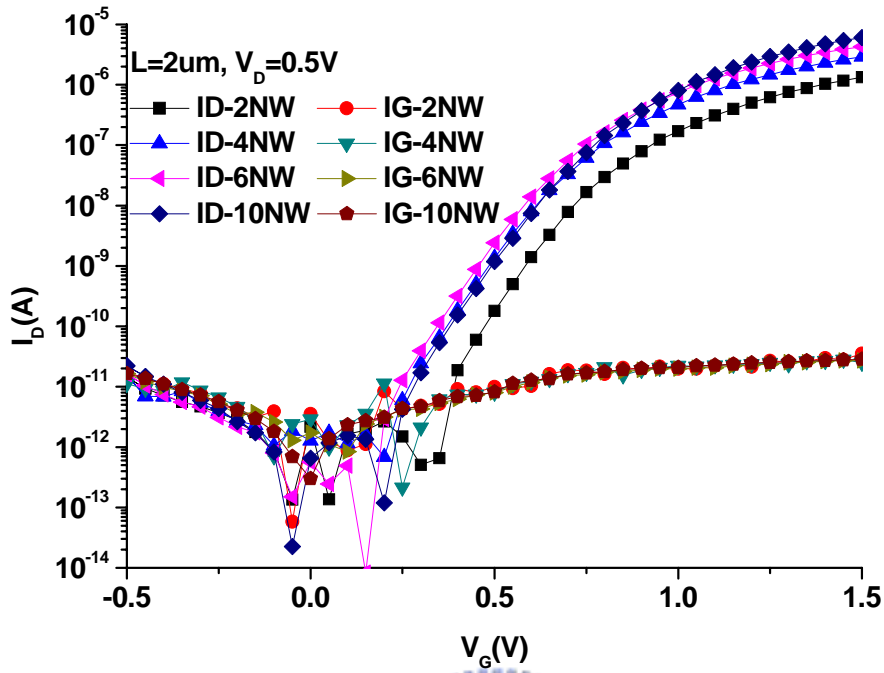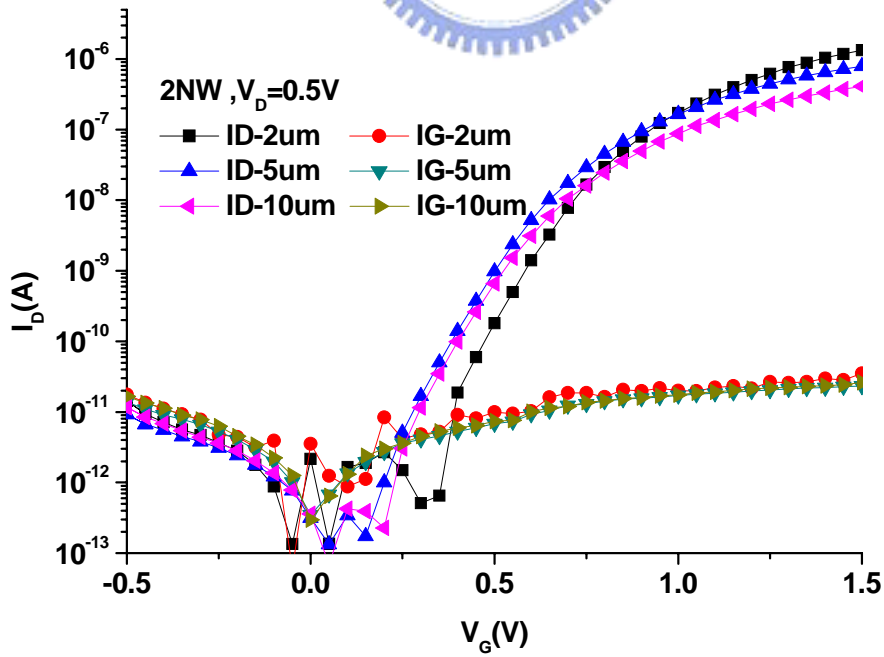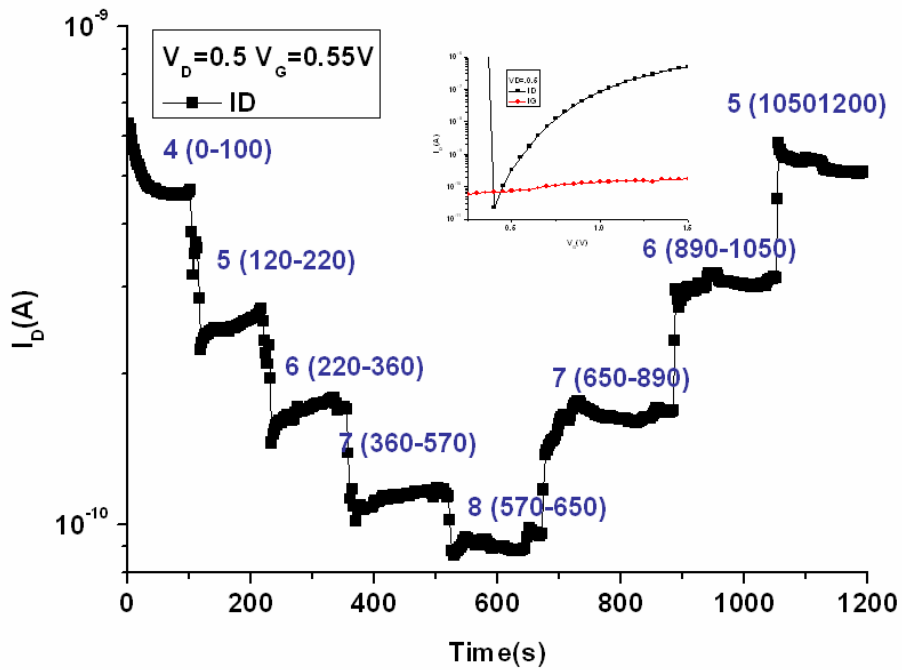
Figure 3- 13：Real-time detection of the drain current for unmodified poly-Si nanowire for difference pH PBS(10mM).
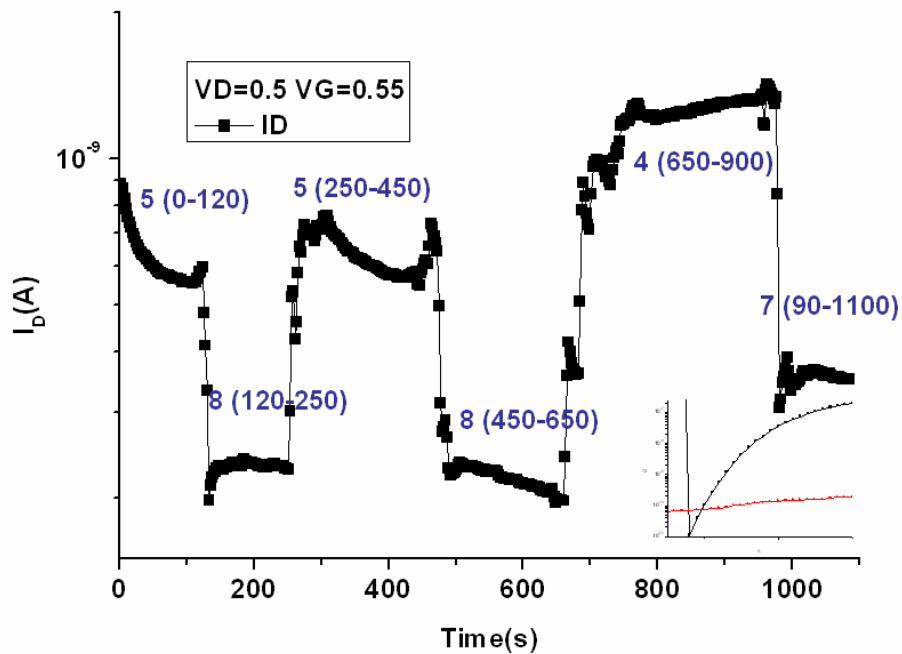

Figure 3- 14：Real-time detection of the drain current for unmodified poly-Si nanowire for difference pH PBS (10mM).
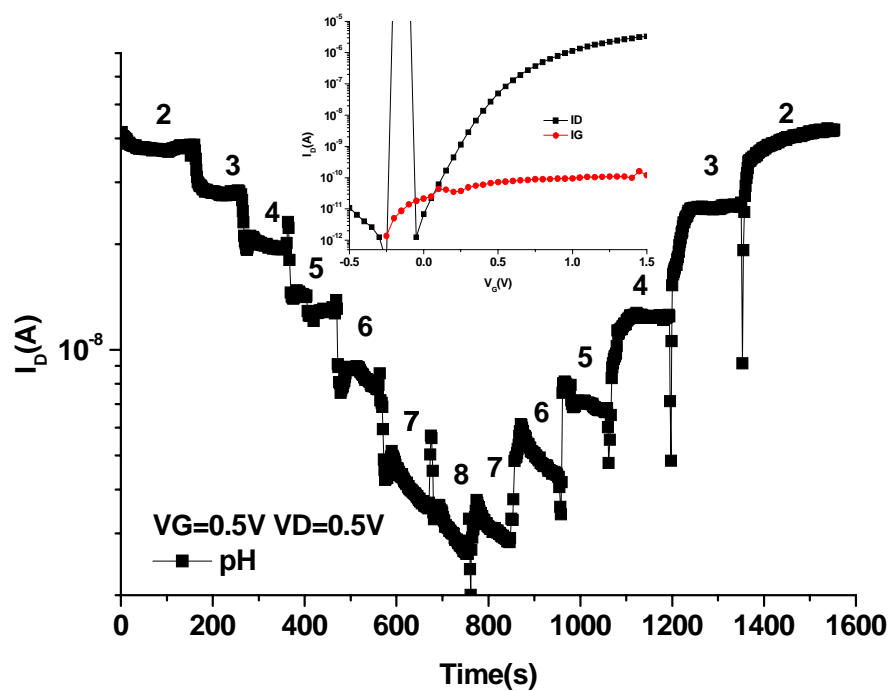
Figure 3- 15：Real-time detection of the drain current for APTES modified poly-Si nanowire for difference pH PBS(10mM).

Figure 3- 16：The microflow system.

Figure 3- 17：Schematics diagram of the interfacial charge trapping mechanism in which -SiOH is deprotonated to –SiO⁻. [10]

Figure 3- 18：Schematics diagram of the interfacial charge trapping mechanism. Zoom of the APTES-modified SiNW surface. [7]
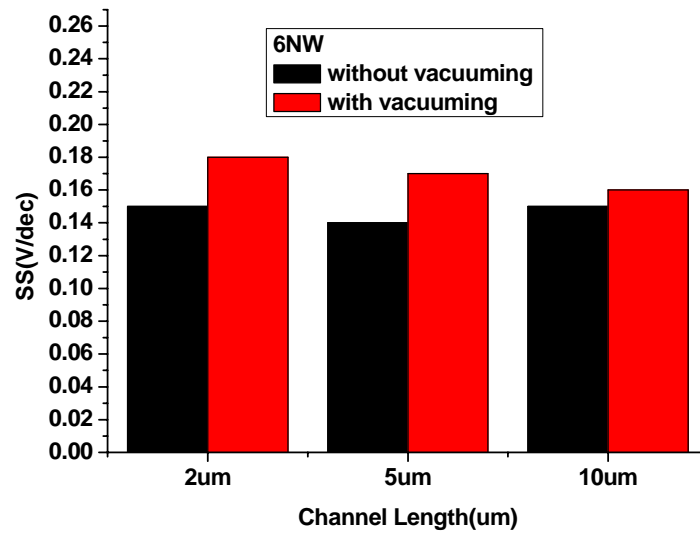
Figure 3- 19：Transfer characteristics of SS of device C as a function of channel length.

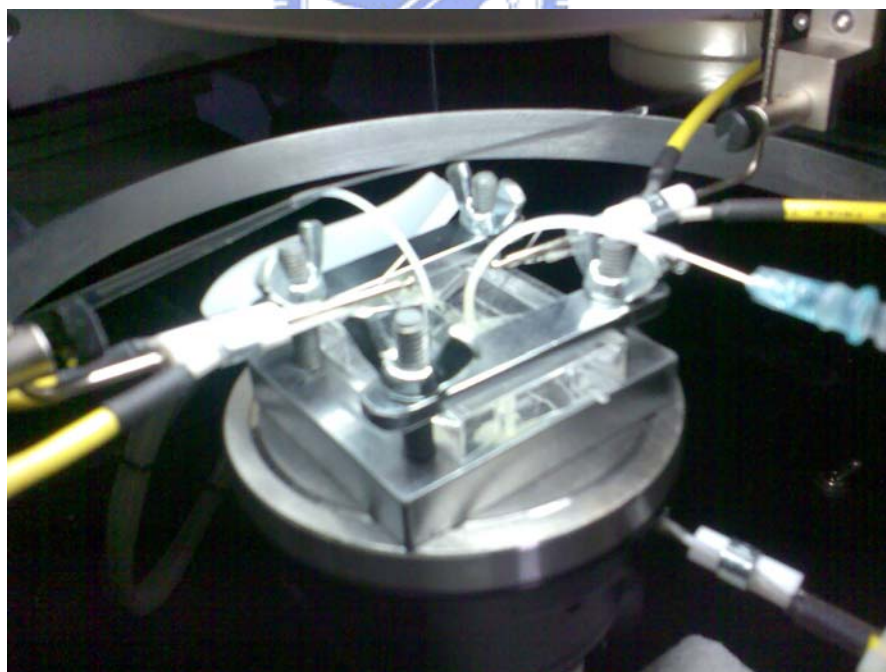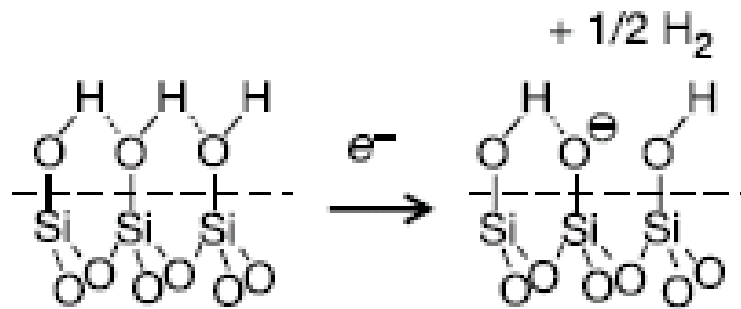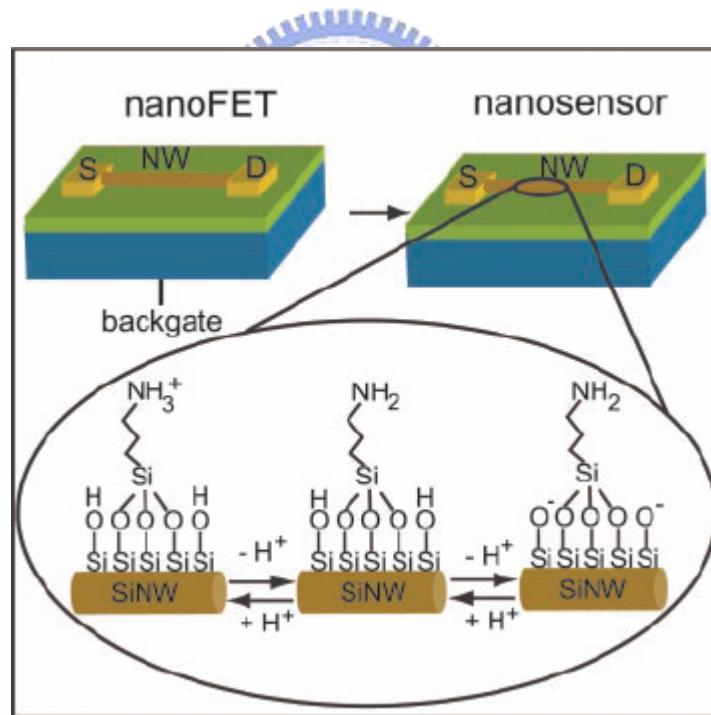Table 3- 1：Summarizes the measured and extracted parameters of normalized on current from the device C (channel length = 2um, V_{G}-V_{th}=0.7V, V_{D}=0.5V).

Normalized On Current	NW×2	NW×4	NW×6	NW×10
Air	7.98E-8	2.78E-08	2.58E-08	2.55E-8
Water	3.08E-7	2.87E-7	2.81E-7	2.82E-7

Table 3- 2：Summarizes the measured and extracted parameters from the device C.

	Channel length	Vth(V)	SS(V/dec)
NW×2	2um	0.5	0.16
	5um	0.35	0.16
	10um	0.37	0.15
NW×4	2um	0.42	0.14
	5um	0.51	0.14
	10um	0.5	0.15
NW×6	2um	0.52	0.14
	5um	0.36	0.14
	10um	0.29	0.24
NW×10	2um	0.49	0.15
	5um	0.53	0.14
	10um	0.56	0.15

Chapter 4：Conclusion

In this thesis, we have successfully fabricated poly-Si NWFET with various numbers of channels and various channel length. Well-behaved device characteristics are obtained in either air or aqueous environment. Three types of NW devices formed on the surface of different insulator were characterized. Among them, the split of device C which was formed on the surface of a nitride capping was found to be most reliable and suitable for bio-logical sensing application. This can be attributed to the high etch selectivity between nitride and the other surface materials (e.g., nitride and oxide), so that the NW surface could be reliably exposed to the environment with the wet etch treatment. In addition to exhibiting good device characteristics in terms of lower threshold voltage and steeper subthreshold slope, clear water passivation is also observed in the device C split.

We also demonstrated the effectiveness of the poly-Si NWFET used for pH-sensor application. In this regard, we carried out real-time measurements to detect the difference in pH PBS of the test solutions. The poly-Si NW devices are either modified or not with APTES. The test devices with APTES-modified nanowire surface show more steady performance than the unmodified one, especially while we pumping PBS with a faster rate.

APPENDIX 1：The Protocol for Prepare 10mM PBS with Difference pH PBS.

Making a phosphate buffer solution is by phosphoric acid. Because of the phosphoric acid has multiple dissociation constants, which are at 2.15, 6.86 and 12.32. The buffer is most commonly prepared at pH 7 using monosodium phosphate and its conjugate base, disodium phosphate.

1. Prepare the solution by mixing 10×10^{-3} moles of monosodium phosphate and 10×10^{-3} moles of disodium phosphate in a little less than a liter of water.

2. Then uniform-stir by hot plate with stirring bar.

3. Check the pH using a pH meter and adjust the pH as necessary using hydrochloric acid or sodium hydroxide.

4. Once you have reached the desired pH, add water to bring the total volume of phosphoric acid buffer to 1 L.

APPENDIX 2：Defined the Ka and pKa

K_a is called the acid-dissociation constant, and its value indicates the relative strength of the acid. It is the equilibrium constant for a chemical reaction known as dissociation in the context of acid-base reactions. For convenience, we will always write such reaction as shown in below equation：

$$HA \Leftrightarrow A^- + H^+$$

Moreover, the stronger the acid, the more it dissociates, giving a larger value of K_a. Acid-dissociation constants vary over a wide range. Strong acids are almost completely ionized in water, and their dissociation constants are greater than 1. The strength of acids is usually expressed in terms of the pK_a value：

$$pK_a = -\log K_a$$

Because pK_a is the negative logarithm of K_a, a numerically small value of pK_a corresponds to a strong acid, and a numerically large value to a weak acid. Some acids, such the phosphoric acid, are capable of losing more than one proton. We called polyprotic acids. The successive dissociation involve separate steps, with separate pK_a values, hence, the PBS exist in several different states of ionization, such as H_3PO_4 (phosphoric acid), $H_2PO_4^-$ (dihydrogen phosphate ion), HPO_4^{2-} (monohydrogen phosphate ion).

APPENDIX 3：The protocol of Modfied the poly-Si nanowire with APTES

1、Setup microfluidics apparatus for separated the water between the pad and the NW channel that shown in Figure 2- 5.

2、For cleaning NW channel, apply the syringe to pump 0.3ml ethanol for three times.

3、Adding 2% ethanol solution of APTES by the syringe to pump the tube.

4、After waiting for 30 minutes, then cleaning by 0.3ml ethanol for three times.

5、Take apart the microfluidics apparatus then put the chip on the heater of $120^{\circ}C$ for 5

minutes.

APPENDIX 4：The pKa of Silicon Nitride

Accurate values for the dissociation constants (pK_a values) of the surface ionic groups on silicon nitride are not available, but Auger and XPS studies indicate that there is a large amount of oxygen bonded to silicon on the surface, indicating the presence of silylamine (basic) and silanol (acidic) groups. Force measurements between silicon nitride surfaces further indicate that the silylammonium groups become deprotonated (uncharged) at a pH of 8-10. Conclusive values for the dissociation constant of the silanol group are not available, but the existence of a net neutral surface at pH 6-7 indicates that the pK of this group is below 6. (Chavez, P., Ducker, W., Israelachvili, J., and Maxwell, K., *Langmuir* 1996. **12**, 4111-4115)

簡歷

姓名：魏若芬

出生日期：民國七十二年十二月十五日

住址：新竹縣湖口鄉錦州一街九號

學歷：

國立竹北高中　資訊科	1999/9　–　2002/6
國立雲林科技大學　電子工程系	2002/9　–　2006/6
國立交通大學　生物醫學所	2006/9　–　2009/6

論文題目：

元件製程對於多晶矽奈米線場效電晶體水測電性影響之分析

Fabrication Process and its Effects on the Electric Characteristics of Poly Crystalline

Silicon Nanowrie Filed Effect Transistor in Aqueous Solution